Structural and functional impact of the H5 hemagglutinin expression into a NDV vector vaccine backbone

Duchatel Victoria,[a]# Steensels Mieke,[a] Verleysen Eveline,[b] Ingrao Fiona,[a] Mast Jan,[b] and Lambrecht Bénédicte[a]

[a]Service of Avian Virology and Immunology, Sciensano, Brussels, Belgium

[b]Service of Trace elements and nanomaterials, Sciensano, Brussels, Belgium

Running Head: Structure and functions of the rNDV-H5 vaccine

#Address correspondence to Victoria Duchatel, victoria.duchatel@sciensano.be

Word count for abstract: 192 + 120

Word count for text: 3451

ABSTRACT

To overcome some of the shortcomings of classical whole virus avian influenza (AI) inactivated vaccines, recombinant vector vaccines, such as recombinant Newcastle disease virus (NDV) vaccines expressing the immunogenic H5 hemagglutinin of AI (rNDV-H5), have been developed. The impact of H5 insertion and surface expression on NDV structure and functionality of a specific bivalent rNDV-H5 vaccine was investigated here.

Structural analysis by immunogold labeling demonstrated the impact of the H5 expression on the surface expression of the rNDV-H5 glycoproteins resulting in a decreased and increased number of fusion (F) and hemagglutinin-neuraminidase (HN) glycoproteins, respectively, compared with the NDV LaSota parental strain. Accordingly, increased hemagglutinating and neuraminidase activities were observed for the rNDV-H5 vaccine.

Functional analysis by monoclonal antibody (mAb) neutralization demonstrated H5 involvement in the rNDV-H5 entry pathway by a reduced *in vitro* infectivity in the presence of neutralizing H5-specific mAb and confirmed the major role of the F glycoprotein in the rNDV-H5 entry pathway as F-specific mAb neutralization resulted in a more important decrease of rNDV-H5 infectivity. However, a significantly lower impact of F-neutralization on rNDV-H5 infectivity was observed compared with the parental strain, confirming the H5-involvement in the rNDV-H5 entry.

IMPORTANCE To prevent economic loss in the poultry industry, vaccination against two major treats, Newcastle Disease Virus (NDV) and Avian Influenza Virus (AIV), is one of major strategy. However, despite intense vaccination campaigns, ND continues to circulate, and AI vaccination expresses shortcomings. In consequence, bivalent vaccines improving simultaneously AI and ND protection in poultry are developed, and tested for their protective

effect while their inherent characteristics are scarcely evaluated. The significance of this paper is to evaluate the impact of the H5 insertion on the NDV structure and functionality in comparison to the parental NDV vaccine, using the rNDV-H5 from Lohmann as material. This advanced characterization helps to better understand the underlying mechanisms of vaccine entry and could help improving vaccination.

INTRODUCTION

Newcastle disease (ND) and highly pathogenic avian influenza (HPAI) are two highly contagious and economically devastating notifiable diseases of major concern to the poultry industry (1). Despite intensive vaccination campaigns in most parts of the world, ND continues to circulate and cause outbreaks (2). Since early 2000, the epizootic Asian clade 1 HPAI H5N1 virus gradually spread from Asia to Europe via wild bird movement and bird trade (3). Meanwhile, HPAI H5 descendants continued to evolve, causing epizootics around the world and becoming endemic in some Asian and African countries, resulting in a continuous threat to the poultry sector (4). Although, whole virus inactivated AI-vaccines have demonstrated efficacy in the past, the use of live replicating vaccines induce a broader range of immune responses including humoral, cell-mediated, and mucosal immunity to protect against homologous and heterologous clades of HPAI H5 (5).

The continued presence and threat imposed by both these avian viruses, emphasize the need for further reinforcement of existing biosafety measures, enhanced surveillance, and improvement of vaccination programs (6, 7). In this context, bivalent vaccines are valuable candidates to improve simultaneously AI and ND protection in poultry (8, 9). A recombinant ND vaccine that carries a hybrid apathogenic clade 1 HP H5 hemagglutinin (rNDV-H5), developed at the Mount Sinai School of Medicine based on their rNDV/F3aa-chimericH7 work (10), has demonstrated its efficacy in SPF chickens against both homologous and heterologous HPAI H5 (11–14) and velogenic ND challenges (13).

The H5-expression at the surface of rNDV-H5 virions of this experimental vaccin has previously been confirmed by immunofluorescence (11) and immunogold electron microscopy (11, 15). However, the impact of the H5 insertion on the ND virus (NDV) surface glycoprotein

organization and the vector life cycle needed further investigations. Para- and Orthomyxoviruses, represented here by NDV and AI virus (AIV) respectively, enter cells by binding to sialic acid receptors using the HN and the hemagglutinin glycoproteins, respectively. To infect cells, NDV uses a pH-independent entry pathway involving the F glycoprotein for fusion with the cell membrane, while binding to the receptor and release of newly formed budding virions rely on the HN glycoprotein (16, 17). For AIV, the hemagglutinin glycoprotein is essential for the binding to the receptor and the fusion with the endosomal membrane, whereas the release of budding virus particles is mediated through the neuraminidase (NA) glycoprotein (18). AIV enters the cells through a pH-dependent pathway where the acidic pH induces conformational changes in the hemagglutinin glycoprotein exposing the fusion peptide to the endosomal membrane, inducing the release of the genome into the cell's cytoplasm (19). Previous vaccination trials using this specific experimental rNDV-H5 vaccine in the presence of anti-NDV maternal derived antibodies, demonstrated protection against heterologous HPAI H5N1 challenge (15), which resulted in the hypothesis that the rNDV-H5 can enter cells by the involvement of the foreign H5 surface glycoprotein, as already demonstrated for a recombinant NDV-Ebola vaccine (20).

The objective of the present study is to evaluate the structural and biological activities of the rNDV-H5 by i) investigating H5, F and HN glycoprotein expression at the surface and ii) assessing the potential impact of the expression of H5 on the vector binding, entry and release processes.

RESULTS

Evaluation of rNDV-H5 glycoproteins expression

The expression of the H5 protein was confirmed by WesternBlot and revealed a molecular weight of 80 kDa and 75 kDa for rNDV-H5 and HP H5N1, respectively (Figure 1).

To determine whether the H5 insertion on the rNDV-H5 surface impacted the surface glycoprotein organization, the glycoprotein expression of the vaccine strain was analyzed by immunogold electron microscopy (Figure 2a) in comparison to the NDV LaSota parental strain. Labeling of H5 demonstrated a significant higher number of gold particles at the rNDV-H5 surface (4.6±0.7 gold/virion) compared to the NDV LaSota surface background values (0.8±0.2 gold/virion) (Figure 2b). Further, significantly lower F glycoprotein expression was detected at the surface of rNDV-H5 (4.3±0.3 gold/virion) compared to NDV LaSota (8.4±0.5 gold/virion). In contrast, a significantly higher HN expression was revealed at the rNDV-H5 surface (25.8±1.4 gold/virion) compared to the NDV LaSota reference (18.4±1.9 gold/virion) (Figure 2b).

Evaluation of the rNDV-H5 HA and NA activities

The HA activity of serially diluted vaccine isolates demonstrated an activity of $10^{4.79}$ TCID50/ml and $10^{5.52}$ TCID50/ml for rNDV-H5 and NDV LaSota, respectively.

The comparison of the NA activity of the rNDV-H5, 42582.2 RFU, and the NDV LaSota, 7424.1 RFU, at a concentration of $10^{5.59}$ TCID50/ml represents a 5.7 times difference in activity (Figure 3).

Investigation of the impact of the H5 insert on the rNDV-H5 entry pathway

VN test

The anti-F, anti-HN, and anti-H5 mAbs VN titers are displayed in Figure 4. The anti-F mAb VN titer for NDV LaSota and rNDV-H5 were comparable, 0.99±0.09 µg/ml versus 0.86±0.10 µg/ml, respectively. The VN titer of the anti-HN mAb for rNDV-H5 infection (1.56±0.21 µg/ml) was

two times higher than for the NDV LaSota infection (0.70±0.08 µg/ml). Although it possesses a VN titer for the clade 1 HPAI H5N1 virus of 1.56±0.21 µg/ml confirming the neutralizing capacity of the mAb used (data not shown), the anti-H5 mAb demonstrated no neutralizing capacity against the rNDV-H5. The H5-neutralization was complete for clade 1 HPAI H5N1 infection (data not shown), while no aspecific neutralization of the NDV LaSota infectivity was confirmed (Figure 5a).

Cytometry-based neutralization assay

An incomplete neutralization of the rNDV-H5 was demonstrated by both anti-F and anti-H5 labeling with a decrease of 6.97±0.11 % and 8.64±1.11 %, respectively (Figures 5a). Viral neutralization by F-specific mAb prior to cell infection (Figure 5b) revealed a statistically significant reduction of NDV LaSota infectivity of 79.14±2.55 %. The rNDV-H5 F-neutralization also demonstrated a significant decrease in both anti-F (65.84±0.99 %) and anti-H5 (11.40±0.67 %) labeling. The decrease observed in viral infectivity after F-specific mAb neutralization was lower for the rNDV-H5 than the NDV LaSota, with statistically more CEFs infected by the rNDV-H5 at a range of 13.93±0.19 %.

Sequence analysis of the H5 and HN genes of the rNDV-H5

Identical nucleotide sequences were observed between the hybrid H5 and the native H5 from HPAI H5N1 clade 1, apart from the engineered attenuated cleavage site and the NDV F-replaced CT and TM domain of the hybrid H5.

For the HN sequence a unique mutation was detected in the HN from rNDV-H5, leading to a S521R change in its amino acid sequence compared to the NDV LaSota HN.

DISCUSSION

The rNDV-H5-vaccine, obtained by reverse genetics from a common LaSota vaccine strain, expresses the H5 ectodomain from a HPAI H5N1, with modified LP-cleavage site and fused with the NDV-F TM and CT domains. The hybrid state between F and H5 is possible due to their similarities as homotrimeric class I proteins (21, 22). The replacement of the H5 TM (25 amino acids) (23) and CT (10 amino acids) (24) domains coding sequences by those of the NDV F glycoprotein, of 21 and 31 amino acids, respectively (25, 26), corresponds to a 17 amino acids increase with a weight of 2.16 kDa. By Western blot, this increased molecular weight of the hybrid H5 protein was demonstrated in comparison with the native clade 1 H5 protein.

The surface expression of the hybrid H5 was confirmed by immunogold electron microscopy for the rNDV-H5 vaccine under investigation as already shown (15) and in accordance with previous studies for similar rNDV-H5 vaccines (11, 12, 27). This accurate and highly sensitive method revealed a reduced number of F and increased number of HN incorporation at the virion surface compared with the parental LaSota strain (Figure 6a). Due to the introduction of the H5 gene between phosphoprotein (P) and matrix (M) genes, a lower expression of F and HN proteins, can be expected as they are downstream from the 3’end reducing their transcription level (28, 29). However, here a differential impact of H5 incorporation on F and HN glycoproteins surface expression was observed, indicating that the reduction of the expression of F at the surface can be rather explained by competition between the CT domains of hybrid H5 and the F glycoproteins for their incorporation into the virion, as suggested earlier (11). It was previously demonstrated that the NDV F interacts with HN and nucleoprotein (NP) without direct M interaction for surface incorporation (30). The stalk region of HN was mapped to be the site of interaction with the second heptad repeat domain (HRB) (31), a membrane-proximal domain of F (32), which is not present in the hybrid H5. Therefore, the H5 hybrid incorporation

is more likely based on an interaction with NP. The surface incorporation of HN involves interaction with the F HRB domain (31) and M (30), moreover interaction with NP is suggested (30). Further research is needed to evaluate the interaction between HN and other viral proteins in terms of HN surface incorporation. To ensure infectivity, the balance between neuraminidase and binding activities has to be maintained (33). In this study, increases of both the HA and NA activities of the rNDV-H5 were measured by classical activity tests. These higher activities can primarily be linked to the observed increased HN surface incorporation while the H5 surface expression can only be responsible for the increased HA activity. The influence of the detected HN S521R mutation, currently undescribed, on the neuraminidase activity is probably limited being far away from the receptor binding and neuraminidase activity site (34). On the contrary, this mutation could be involved in the increase of HA activity as it is located near the R516 amino acid, involved in the formation of the second sialic acid binding site (site II) (35). For the human parainfluenza virus 1 HN glycoprotein, sharing similar molecular structure with the NDV HN but lacking a site II, a N523D mutation induces the formation of this site II (36). The similar S521R mutation detected here in the rNDV-H5 HN, from a polar to a positively charged amino acid, could impact the activation of the rNDV-H5 HN site II. Further research is needed to validate this site II activation hypothesis for the rNDV-H5.

The functionality and participation of both the hybrid H5 and the NDV glycoproteins in the rNDV-H5 entry were demonstrated by flow cytometry-based neutralization assays. This observation is in line with a previous observation of a recombinant NDV vector expressing an Ebola surface glycoprotein, that used the Ebola micropinocytosis as major internalization route for cell entry, indicating that a foreign surface glycoprotein could strongly alter or completely change the entry pathway of the NDV virus (20). Here, only a partial neutralization of the rNDV-

H5 entry by the anti-H5 mAb was observed, indicating that the H5-entry pathway is functional but not the major entry pathway (Figure 6b). The higher but incomplete neutralization of the rNDV-H5 entry by the anti-F mAb, observed for both anti-F and anti-H5 labeling, confirmed the NDV-entry pathway as the primary route of infection for the rNDV-H5 and the involvement of the H5. Previous studies already demonstrated the efficiency of pH-independent endosomal entry for the NDV LaSota as a secondary route of infection due to the absence of pH-induced conformational change in NDV glycoproteins (16, 17). The rNDV-H5 entry pathway could occur by receptor recognition mediated by HN and H5, afterwards inducing a principal fusion at the cell membrane with F and, allowing a secondary fusion at the endosomal membrane with H5 at acidic pH or with F without pH-involvement (Figure 6b). Therefore, it was hypothesized that the endosomal entry, mediated by the hybrid H5, could modulate the early immune response with a broader stimulation of intracellular vesicle sensors such as TLR3 and TLR7, in parallel to a stimulation of cytoplasmic sensors like MDA5 and LGP2 (37). Additional work is necessary to investigate the early immune response induced by the NDV and rNDV-H5 infection *in vitro* in order to validate, or not, this hypothesis.

In conclusion, this study contributes to a better understanding of the mechanisms of entry of a bivalent rNDVH5. For the first time, it was shown that the expression of the hybrid H5-insert on the surface of the rNDV-H5 particles affect the expression of NDV glycoproteins and by consequence the biological characteristics of the rNDV-H5. The functionality of the H5 entry pathway and its use as a secondary entry pathway was also demonstrated. However, their impact on the induced immune response should be investigated further.

MATERIALS AND METHODS

Vaccine and viruses

The rNDV-H5 vaccine, expressing a modified H5 ectodomain from a human HPAI H5N1 clade 1 strain (A/Vietnam/1203/04), and the parental NDV LaSota were provided by Lohmann Animal Health GmbH (Germany) (14). The H5 insert of the rNDV-H5 had been modified into a low-pathogenic version to ensure vaccine safety (12). In addition, to assure surface expression, and therefore the immunogenic response, the H5 transmembrane (TM) domain and cytoplasmic tail (CT) were replaced by those of the NDV F glycoprotein (10, 11). The H5 gene was inserted between the P and M genes of the NDV genome identified as the optimal insertion site for gene expression (38).

As clade 1 representative, the HPAI H5N1 A/Crested-eagle/Belgium/01/2004 strain, isolated from two illegally imported crested hawk eagles in 2004 in Belgium (39), was used as H5 control for Western blot, neutralization, and flow cytometry assays.

All vaccines and virus were amplified by inoculation into the allantoic cavity of 9-11 day old embryonated specific pathogen free (SPF) eggs. Five days after inoculation or at embryonic death, allantoic fluids were harvested and the isolates were titrated on primary chicken embryo fibroblasts (CEFs) (40) to determine the tissue culture infectious dose (TCID50/ml) (41).

For Western blot and immunogold electron microscopy analysis, viral strains were purified by differential centrifugation on a sucrose gradient, as previously described (42). The total protein concentration of purified viruses was determined with the bicinchoninic acid assay Kit (ThermoFisher Scientific, Massachusetts, USA) and was expressed in µg/ml.

Monoclonal antibodies

The applied mAb's directed against NDV and AIV glycoproteins were *in house* produced: mouse anti-NDV F 1C3 at 1.14 mg/ml (IgG1) (43); mouse anti-NDV HN 4D6 at 1.26 mg/ml (IgG2a) (43); and mouse anti-AIV H55A1 at 1.05 mg/ml (IgG1) (44).

Western blot

H5-expression was analyzed by Western blot as previously described (45). Briefly, each sample was tested at a concentration of 200 µg/ml and separated on a 12 % polyacrylamide gel. After transfer onto a nitrocellulose membrane and saturation with tween tris-buffered saline (TTBS) – 5 % bovine serum albumin (BSA) solution (Sigma Aldrich, Missouri, USA) overnight at 4°C, the H5 was detected using the 5A1 anti-H5 mAb diltuted 1:500 in TTBS – 1 % BSA for 1h at room temperature (RT) on a shaking table. The H5 was visualized using biotinylated anti-mouse IgG secondary antibody diluted 1:10000 in TTBS – 1 % BSA reacting with streptavidin-alkaline phosphatase conjugate (Sigma Aldrich) and revealed with SIGMAFAST BCIP/NTB reagent (Sigma Aldrich).

Visualization of rNDV-H5 surface glycoproteins by immunogold electron microscopy

Glycoprotein surface expression on rNDV-H5 and NDV LaSota was evaluated by the previously described immunogold labeling method (15) with minor modifications. Briefly, pioloform/carbon-coated copper grids (Agar Scientific, Stansted Essex, England) were pretreated for 10 min at RT with Alcian blue 8G (Gurr Microscopy Materials, Poole, England) solution at 1 % v/v in water. The rNDV-H5 and NDV LaSota were diluted in PBS to a final concentration of 75 µg/ml and adsorbed for 10 min at RT onto pretreated grids. Anti-F, anti-HN and anti-H5 mAbs at 1:50 dilution in PBS supplemented with 2 % of goat serum (v/v) were then adsorbed to the grid. The irrelevant anti-IFNγ 3D5 mAb (1.4 mg/ml) (44) was used as a negative control for immunogold labeling. The number of gold particles at the virions' surface was assessed in 50

representative virions. Images of immunogold-labeled virions were acquired on a Tecnai G2 Spirit electron microscope (FEI, Eindhoven, Netherlands) using bright field transmission electron microscopy mode. To take in account the pleomorphism of NDV viruses (46), the surface of each virion was determined by image analysis and the number of gold labels were expressed per 55000 nm^2, which was the mean surface of the analysed virions, estimating the number of gold particles per virion (#gold/virion).

Hemagglutinating (HA) and neuraminidase (NA) activity tests

The HA activity of NDV LaSota and rNDV-H5 was evaluated by the standard hemagglutination assay (47), for which the last viral dilutions determines the HA titer.

The NA activity of NDV LaSota and rNDV-H5 was determined using the NA-fluor Influenza Neuraminidase Assay kit (Applied Biosystems, CA, USA) according to manufacturer's recommendations and expressed as Relative Fluorescent Unit (RFU).

Virus neutralization (VN) test and flow cytometry-based neutralization assay

A culture of primary CEFs was seeded at a concentration of 5 10^5 CEFs/ml in Leibovitz's L15/McCoy's 5A (1:1) medium (Gibco, ThermoFisher Scientific, USA) supplemented with 2 % fetal calf serum in 96-well plates for VN test or in T75 culture flask for flow cytometry (16, 48) assay. Cells were incubated (37 °C, 5 % CO_2) for 24h to reach 80 % of confluence.

VN test

Two-fold serial dilutions of an initial 5 µg/ml concentration of the mAbs were incubated for 3h at 37 °C with NDV LaSota or rNDV-H5 in medium supplemented with L-1-tosylamido-2-phenylethylchloromethyl ketone (TPCK) – trypsin (Sigma Aldrich) at a final concentration of 50 ng/ml. Subsequently, CEFs monolayers were infected with 100 µl of the vaccine-mAbs

complexes at a multiplicity of infection (MOI) of 0.01. After 24 h of incubation at 37 °C, 5 % CO_2, 100 µl of fresh medium supplemented with TPCK-trypsin was added to boost viral replication. CEFs were monitored daily over a 7 day period for the presence of a cytopathic effect (CPE). The VN titer of each mAb was expressed as the last mAb concentration where no CPE was observed.

Flow cytometry assay

The rNDV-H5, NDV LaSota or H5N1 strains were pre-incubated for 90 min at 37 °C with specific anti-H5 or anti-F mAb, concentration diluted in medium based on the VN results for each mAb. Subsequently, the CEFs monolayers were infected with 4 ml of the virus-mAbs complexes at a MOI of 0.01 and incubated at 37 °C. The infectious medium was replaced after 1h by 4 ml of complete medium supplemented with TPCK-trypsin and mAbs. After 3h at 37 °C, the medium was replaced with 10 ml of fresh medium supplemented with TPCK-trypsin, and incubated for 24h at 37 °C. CEFs were detached by Trypsin-EDTA 0,25 % (ThermoFisherScientific) and 10^6 infected cells for each condition were labeled for 30 min at 4 °C with either anti-F or anti-H5 primary mAb diluted 1:50. Thereafter, infected cells were labeled for 30 min at 4 °C with secondary anti-mouse IgG1 antibody coupled with fluorescein isothiocyanate (FITC) diluted 1:50 (Southern Biotech, AL, USA). After overnight fixation in BD cytofix (BD-Biosciences, New Jersey,USA) at 4 °C, 10^4 cells were analyzed for each condition using a FACS calibur flow cytometer (BD-Biosciences). To determine the “living cells area”, unlabeled cells were analyzed by Side SCatter (SSC), giving a representation of the granularity, and Forward SCatter (FSC), representing the size, comparison (Figure 4A). The “positive cells area” is determined based on the fluorescence signal of cells labeled with isotype matched

control antibodies. The exact same "living cells area" and "positive cells area" were used for all analysis. The results were expressed as the percentage of living cells post infection.

Sequencing of rNDV-H5 H5 and HN genes

Viral RNA from rNDV-H5 allantoic fluid was extracted using the High Pure Viral Nucleic Acid kit (Roche, Basel, Switzerland) according to the manufacturer's recommendations. The high fidelity One-step RT-PCR kit (Qiagen, Hilden, Germany) was used to obtain cDNA (49) with specifically designed primers to amplify the HN and H5 genes from the extracted RNA (Table 1). The amplified PCR fragments were purified by agarose gel electrophoresis and sequenced using the BigDye Terminator V.3.1 cycle sequencing kit (ThermoFisher Scientific) with specific primers (Table 1). Sequences were analyzed using BioEdit software and compared to the published NDV LaSota (GenBank: AF077761) and H5 from H5N1 A/Vietnam/1203/04 (GenBank: AY818135.1) sequences.

Table 1.

Target gene	Primer name	Sequence	Test
H5	LS 2955F	5'- GCA-TTG-ATC-ATG-TCA-CGC -3'	cDNA amplification
	LS 3435R	5'- CAC AAG TCA AGG CGC TG -3'	
	H5 977F	5'- GAT TAG TCC TTG CGA CTG -3'	Sequencing
	H5 18F	5'- CTT TTT GCA ATA GTC AGT C -3'	
	H5 304F	5'- GTC AAT GAC CTC TGT TAC -3'	
	H5 723F	5'- GAT GGA GTT CTT CTG GAC -3'	
	H5 804R	5'- GTA TGC ATA TTC TGG AGC A -3'	
	LS 3394R	5'- CTT-CTT-CCC-ATC-TCC-TG -3'	
	H5 1092R	5'- TAC CATTCC CTG CCA TC-3'	
	H5 434R	5'- AAT GAG GCT TCA TGA CTG-3'	
HN	Seq_F6	5'- CGG-TTG-TAG-ATG-ACC-AAA-GG-3'	cDNA amplification

	Seq_R3	5’- TGA-GCA-CTG-GCT-GAT-TGT-G-3’	
	Seq_F7	5’- ATT-TTA-TCC-CGG-CGC-CTA-3’	Sequencing
	Seq_F8	5’- TTC-GTA-TAA-GCC-TGG-ACG-G-3’	

Statistical analyses

Statistical analyses were performed using R 3.0.3 statistical software. Immunogold electron microscopy results were analyzed by non-parametric Kruskal-Wallis test and, for normally distributed values, with one-way analysis of variance (ANOVA). The neutralization assay data were analyzed with Student’s paired *t*-test using permutation. Flow cytometry data were analyzed by ANOVA or by Student’s paired *t*-test with Welch correlation in function of the normality. P-value < 0.05were considered statistically significant.

ACKNOWLEDGMENTS

This work was financially supported by the BELVIR-consortium (FNRS, Belgium) and Sciensano.

The authors thank Alexandre Ausloos, Marc Boschmans, Eva Ngabirano, and Catherine Rasseneur members of the Sciensano’s ‘avian virology and immunology’ team and Marina Ledecq part of the Sciensano’s ‘trace elements and nanomaterials’ service for their help and support in the realization of the experiments performed in this paper. A special thanks is addressed to Lohmann Animal Health GmbH (Germany) who provided the rNDV-H5 and the NDV LaSota vaccines for this research.

REFERENCES

1. Alexander DJ. 2000. Newcastle disease and other avian paramyxoviruses. Rev Sci Tech 19:443–62.

2. Senne DA, King DJ, Kapczynski DR. 2004. Control of Newcastle disease by vaccination. Dev Biol (Basel) 119:165–70.

3. Sonnberg S, Webby RJ, Webster RG. 2013. Natural history of highly pathogenic avian influenza H5N1. Virus Res 178:63–77.

4. Brown IH. 2010. Summary of Avian Influenza Activity in Europe, Asia, and Africa, 2006–2009. Avian Dis 54:187–193.

5. Jang H, Elaish M, Mahesh KC, Abundo MC, Ghorbani A, Ngunjiri JM, Lee CW. 2018. Efficacy and synergy of live-attenuated and inactivated influenza vaccines in young chickens. PLoS One 13:1–22.

6. Krammer F, Palese P. 2015. Advances in the development of influenza virus vaccines. Nat Rev Drug Discov 14:167–82.

7. De Vries E, Guo H, Dai M, Rottier PJM, Van Kuppeveld FJM, De Haan CAM. 2015. Rapid emergence of highly pathogenic avian influenza subtypes from a subtype H5N1 hemagglutinin variant. Emerg Infect Dis 21:842–846.

8. Peyre M, Fusheng G, Desvaux S, Roger F. 2009. Avian influenza vaccines: a practical review in relation to their application in the field with a focus on the Asian experience. Epidemiol Infect 137:1–21.

9. Tripp RA, Mark Tompkins S, Tompkins SM, Mark Tompkins S. 2014. Virus-vectored influenza virus vaccines. Viruses 6:3055–3079.

10. Park M-S, Steel J, García-Sastre A, Swayne D, Palese P. 2006. Engineered viral vaccine constructs with dual specificity: avian influenza and Newcastle disease. Proc Natl Acad Sci U S A 103:8203–8208.

11. Nayak B, Rout SN, Kumar S, Khalil MS, Fouda MM, Ahmed LE, Earhart KC, Perez DR, Collins PL, Samal SK. 2009. Immunization of chickens with Newcastle disease virus expressing H5 hemagglutinin protects against highly pathogenic H5N1 avian influenza viruses. PLoS One 4:1–10.

12. Ge J, Deng G, Wen Z, Tian G, Wang Y, Shi J, Wang X, Li Y, Hu S, Jiang Y, Yang C, Yu K, Bu Z, Chen H. 2007. Newcastle Disease Virus-Based Live Attenuated Vaccine Completely Protects Chickens and Mice from Lethal Challenge of Homologous and Heterologous H5N1 Avian Influenza Viruses. J Virol 81:150–158.

13. Veits J, Wiesner D, Fuchs W, Hoffmann B, Granzow H, Starick E, Mundt E, Schirrmeier H, Mebatsion T, Mettenleiter TC, Romer-Oberdorfer A. 2006. Newcastle disease virus expressing H5 hemagglutinin gene protects chickens against Newcastle disease and avian influenza. Proc Natl Acad Sci 103:8197–8202.

14. Lardinois A, Steensels M, Lambrecht B, Desloges N, Rahaus M, Rebeski D, van den Berg T. 2012. Potency of a Recombinant NDV-H5 Vaccine Against Various HPAI H5N1 Virus Challenges in SPF Chickens. Avian Dis 56:928–936.

15. Lardinois A, Vandersleyen O, Steensels M, Desloges N, Mast J, van den Berg T, Lambrecht B. 2016. Stronger Interference of Avian Influenza Virus–Specific Than Newcastle Disease Virus–Specific Maternally Derived Antibodies with a Recombinant NDV-H5 Vaccine. Avian Dis 60:191–201.

16. Sánchez-Felipe L, Villar E, Muñoz-Barroso I. 2014. Entry of Newcastle Disease Virus into the host cell: Role of acidic pH and endocytosis. Biochim Biophys Acta - Biomembr 1838:300–309.

17. Ganar K, Das M, Sinha S, Kumar S. 2014. Newcastle disease virus: Current status and our understanding. Virus Res 184:71–81.

18. Lee CW, Saif YM. 2009. Avian influenza virus. Comp Immunol Microbiol Infect Dis 32:301–310.

19. Edinger TO, Pohl MO, Stertz S. 2014. Entry of influenza A virus: Host factors and antiviral targets. J Gen Virol 95:263–277.

20. Wen Z, Zhao B, Song K, Hu X, Chen W, Kong D, Ge J, Bu Z. 2013. Recombinant lentogenic Newcastle disease virus expressing Ebola virus GP infects cells independently of exogenous trypsin and uses macropinocytosis as the major pathway for cell entry. Virol J 10:331.

21. Russell CJ, Luque LE. 2006. The structural basis of paramyxovirus invasion. Trends Microbiol 14:243–246.

22. Stevens J, Blixt O, Tumpey TM, Taubenberger JK, Paulson JC, Wilson IA. 2006. Structure and receptor specificity of the hemagglutinin from an H5N1 influenza virus. Science 312:404–410.

23. Lin S, Naim HY, Rodriguez AC, Roth MG. 1998. Mutations in the middle of the transmembrane domain reverse the polarity of transport of the influenza virus hemagglutinin in MDCK epithelial cells. J Cell Biol 142:51–57.

24. Zhang J, Pekosz A, Lamb RA. 2000. Influenza virus assembly and lipid raft microdomains: a role for the cytoplasmic tails of the spike glycoproteins. J Virol 74:4634–44.

25. Samal S, Khattar SK, Paldurai A, Palaniyandi S, Zhu X, Collins PL, Samal SK. 2013.

Mutations in the Cytoplasmic Domain of the Newcastle Disease Virus Fusion Protein Confer Hyperfusogenic Phenotypes Modulating Viral Replication and Pathogenicity. J Virol 87:10083–10093.

26. Gravel KA, McGinnes LW, Reitter J, Morrison TG. 2011. The transmembrane domain sequence affects the structure and function of the Newcastle disease virus fusion protein. J Virol 85:3486–97.

27. Ramp K, Veits J, Deckers D, Rudolf M, Grund C, Mettenleiter TC, Römer-Oberdörfer A. 2011. Coexpression of Avian Influenza Virus H5 and N1 by Recombinant Newcastle Disease Virus and the Impact on Immune Response in Chickens. Avian Dis Dig 6:e11–e12.

28. Collins PL, Hightower LE, Ball LA. 1978. Transcription and translation of Newcastle disease virus mRNA's in vitro. J Virol 28:324–336.

29. Yan Y. 2008. Role of Noncoding Regions in Newcastle Disease Virus Replication and Pathogenesis. University of Maryland.

30. Pantua HD, McGinnes LW, Peeples ME, Morrison TG. 2006. Requirements for the assembly and release of Newcastle disease virus-like particles. J Virol 80:11062–11073.

31. Deng R, Wang Z, Mirza AM, Iorio RM. 1995. Localization of a Domain on the Paramyxovirus Attachment Protein Required for the Promotion of Cellular Fusion by Its Homologous Fusion Protein Spike. Virology.

32. Gravel K a, Morrison TG. 2003. Interacting domains of the HN and F proteins of newcastle disease virus. J Virol 77:11040–11049.

33. Tappert MM, Porterfield JZ, Gulati S, Air GM. 2013. Quantitative Comparison of Human

Parainfluenza Virus Hemagglutinin-Neuraminidase Receptor Binding and Receptor 87:8962–8970.

34. Crennell S, Takimoto T, Portner A, Taylor G. 2000. Crystal structure of the multifunctional paramyxovirus hemagglutinin-neuraminidase. Nat Struct Biol 7:1068–1074.

35. Porotto M, Salah Z, DeVito I, Talekar A, Palmer SG, Xu R, Wilson IA, Moscona A. 2012. The Second Receptor Binding Site of the Globular Head of the Newcastle Disease Virus Hemagglutinin-Neuraminidase Activates the Stalk of Multiple Paramyxovirus Receptor Binding Proteins To Trigger Fusion. J Virol 86:5730–5741.

36. Bousse T, Takimoto T. 2006. Mutation at residue 523 creates a second receptor binding site on human parainfluenza virus type 1 hemagglutinin-neuraminidase protein. J Virol 80:9009–9016.

37. Xiang B, Zhu W, Li Y, Gao P, Liang J, Liu D, Ding C, Liao M, Kang Y, Ren T. 2018. Immune responses of mature chicken bone-marrow-derived dendritic cells infected with Newcastle disease virus strains with differing pathogenicity. Arch Virol 163:1–11.

38. Zhao W, Zhang Z, Zsak L, Yu Q. 2015. P and M gene junction is the optimal insertion site in Newcastle disease virus vaccine vector for foreign gene expression. J Gen Virol 96:40–45.

39. Steensels M, Van Borm S, Boschmans M, van den Berg T. 2007. Lethality and Molecular Characterization of an HPAI H5N1 Virus Isolated from Eagles Smuggled from Thailand into Europe. Avian Dis 51:401–407.

40. Shahsavandi S, Ebrahimi MM, Mohammadi A, Zarrin Lebas N. 2013. Impact of chicken-

origin cells on adaptation of a low pathogenic influenza virus. Cytotechnology 65:419–424.

41. Nagy A, Lee J, Mena I, Henningson J, Li Y, Ma J, Duff M, Li Y, Lang Y, Yang J, Abdallah F, Richt J, Ali A, Garc??a-Sastre A, Ma W. 2016. Recombinant Newcastle disease virus expressing H9 HA protects chickens against heterologous avian influenza H9N2 virus challenge. Vaccine 34:2537–2545.

42. Ren X, Xue C, Kong Q, Zhang C, Bi Y, Cao Y. 2012. Proteomic analysis of purified Newcastle disease virus particles. Proteome Sci 10:32.

43. Meulemans G, Gonze M, Carlier MC, Petit P, Burny A, Long L. 1987. Evaluation of the use of monoclonal antibodies to hemagglutinin and fusion glycoproteins of Newcastle disease virus for virus identification and strain differentiation purposes. Arch Virol 92:55–62.

44. Ferreira HL, Lambrecht B, van Borm S, Torrieri-Dramard L, Klatzmann D, Bellier B, van den Berg T, Borm AS Van, Torrieri-dramard AL, Klatzmann BCD, Ferreira HL, Be AD, Bellier B, A TVDB. 2010. Identification of a Dominant Epitope in the Hemagglutinin of an Asian Highly Pathogenic Avian Influenza H5N1 Clade 1 Virus by Selection of Escape Mutants. Avian Dis 54:565–571.

45. Meshkat Z, Roostaee MH, Soleimanjahi H, Hassan Roostaee M, Soleimanjahi H. 2009. Development of a Western Blot Assay for Detection of Antibodies against HSV Using Purified HSV Virions Prepared by Sucrose Density Gradient. Iran J Basic Med Sci 11:215–220.

46. Kortekaas J, Dekker A, de Boer SM, Weerdmeester K, Vloet RPM, Wit AAC de, Peeters

BPH, Moormann RJM. 2010. Intramuscular inoculation of calves with an experimental Newcastle disease virus-based vector vaccine elicits neutralizing antibodies against Rift Valley fever virus. Vaccine 28:2271–2276.

47. Spackman E. 2014. Animal Influenza VirusAnimal Influenza Virus. Springer New York, New York, NY, NY.

48. Kraus AA, Messer W, Haymore LB, De Silva AM. 2007. Comparison of plaque- and flow cytometry-based methods for measuring dengue virus neutralization. J Clin Microbiol 45:3777–3780.

49. Spackman E, Senne DA, Myers TJ, Bulaga LL, Garber LP, Perdue ML, Lohman K, Daum LT, Suarez DL. 2002. Development of a Real-Time Reverse Transcriptase PCR Assay for Type A Influenza Virus and the Avian H5 and H7 Hemagglutinin Subtypes Development of a Real-Time Reverse Transcriptase PCR Assay for Type A Influenza Virus and the Avian H5 and H7 Hemagglutini. J Clin Microbiol 40:3256–3260.

FIGURE LEGENDS

Figure 1. H5 glycoprotein expression detection by Western blot analysis of NDV LaSota, rNDV-H5 and HP H5N1. The B2787 biotinylated molecular weights marker (Sigma-Aldrich) is indicated in kDa on the left.

Figure 2. a) Representative transmission electron micrographs illustrating H5-specific immunogold labeling. Unlabeled rNDV-H5 viral particles can be observed on the left and anti-HN labeled rNDV-H5 particles on the right. b) Immunogold H5, F and HN glycoprotein labeling of sucrose-purified NDV LaSota and rNDV-H5. The number of gold particles were counted and normalized per virion surface unit of 55000 nm^2. Statistical analysis was performed by non-parametric Kruskal-Wallis test and ANOVA test to compare labeling for both strains. Results are expressed as mean ± SEM and statistical significance of differences in mean values are expressed as follows depending on the p-value: *** < 0.001, ** < 0.01, * < 0.1.

Figure 3. rNDV-H5 neuraminidase activity. The selected concentration to compare the activity of both virus was determined based on manufacturer's instructions and corresponds to $10^{5,59}$ TCID50/ml (full bold line).

Figure 4. mAb neutralizing titer for NDV LaSota and rNDV-H5 infectivity. The neutralizing titer of each mAb is the last mAb concentration showing no CPE. Statistical analysis was performed by Student's paired t-test using permutation to compare mAb concentration for both strains. Results are expressed as mean ± SD and differences are expressed as following, depending on the p-value result: *** < 0.001, ** < 0.01, * < 0.1.

Figure 5. a) NDV LaSota, rNDV-H5 and HP H5N1 infectivity post H5-neutralization. b) NDV LaSota and rNDV-H5 infectivity post F-neutralization. Statistical analysis was performed by

ANOVA or by Student's paired t-test with Welch correlation to compare the infectivity with or without neutralization. Results are expressed as mean ± SD and statistical significance of differences in mean values are expressed as follows depending on the p-value: *** < 0.001, ** < 0.01, * < 0.1.

Figure 6. a) Representation of the rNDV-H5 (right) structure in comparison with the parental NDV strain (left). B) Representation of the entry pathway of the rNDV-H5. [Adapted from (17)]

TABLES

Table 1. List of primers. *In house* developed primers were used to perform OneStep RT-PCR detection or sequencing of the H5 or HN genes.

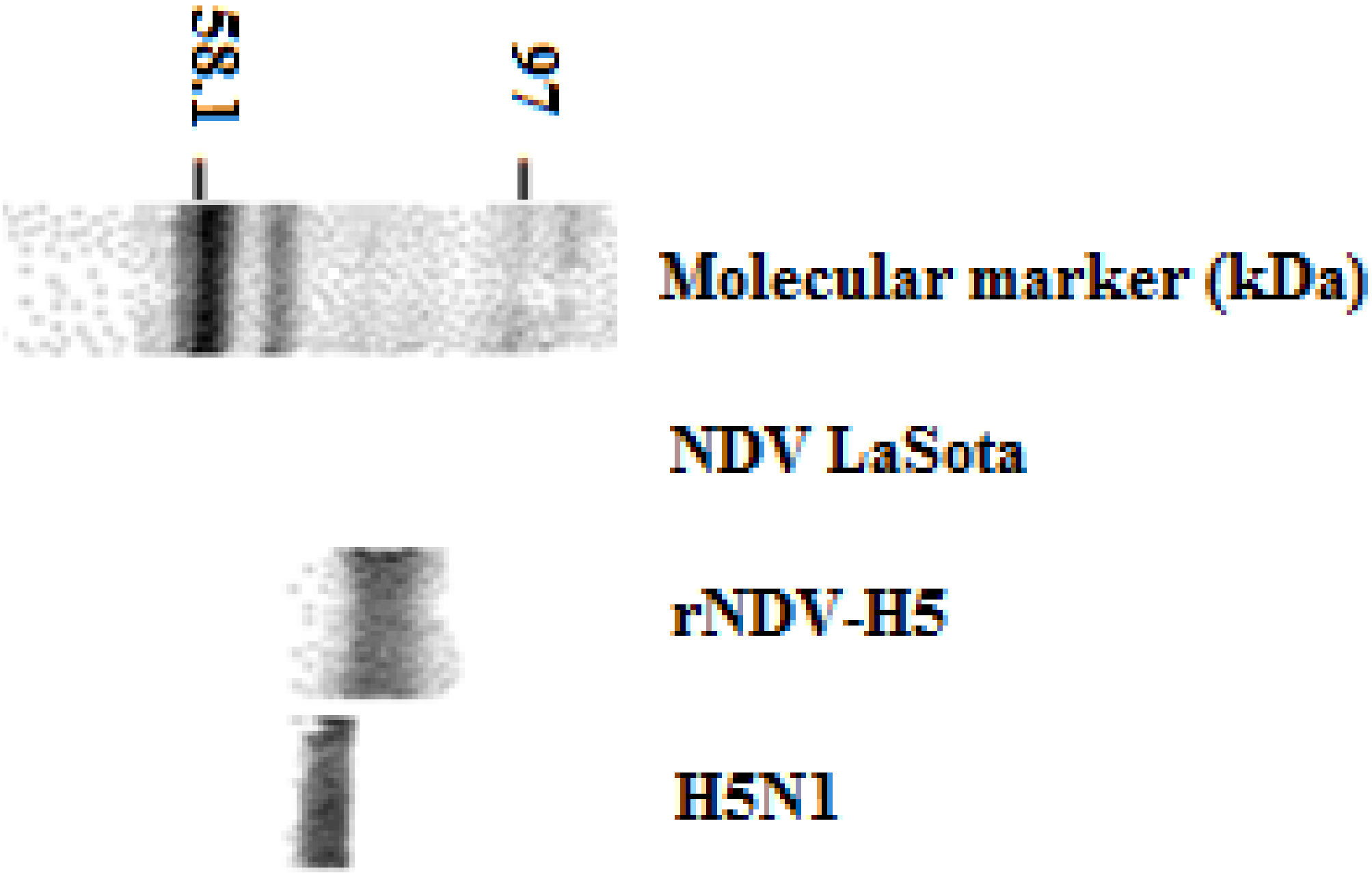
Molecular marker (kDa)
97
58.1
NDV LaSota
rNDV-H5
H5N1

a)

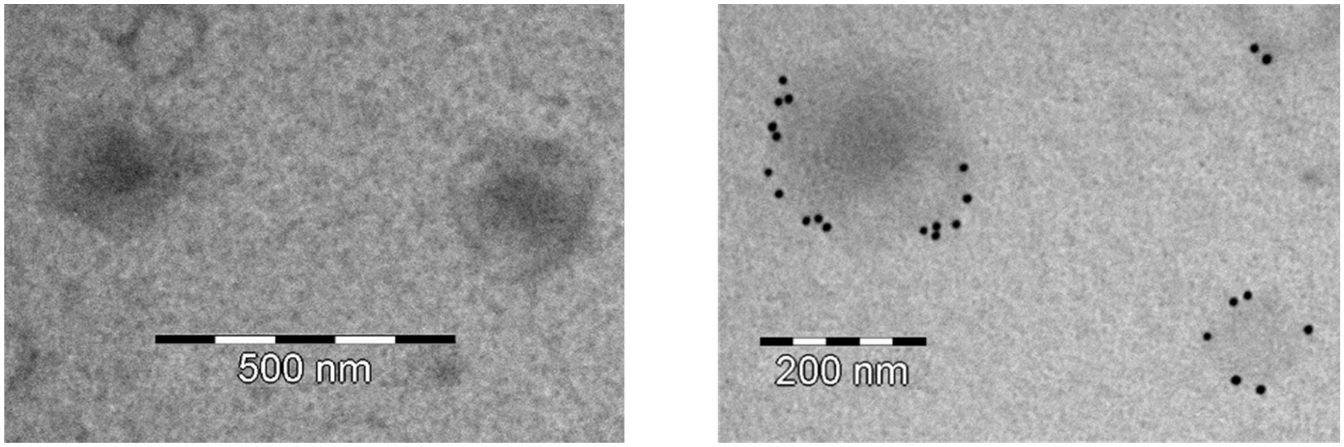
500 nm
200 nm

b)

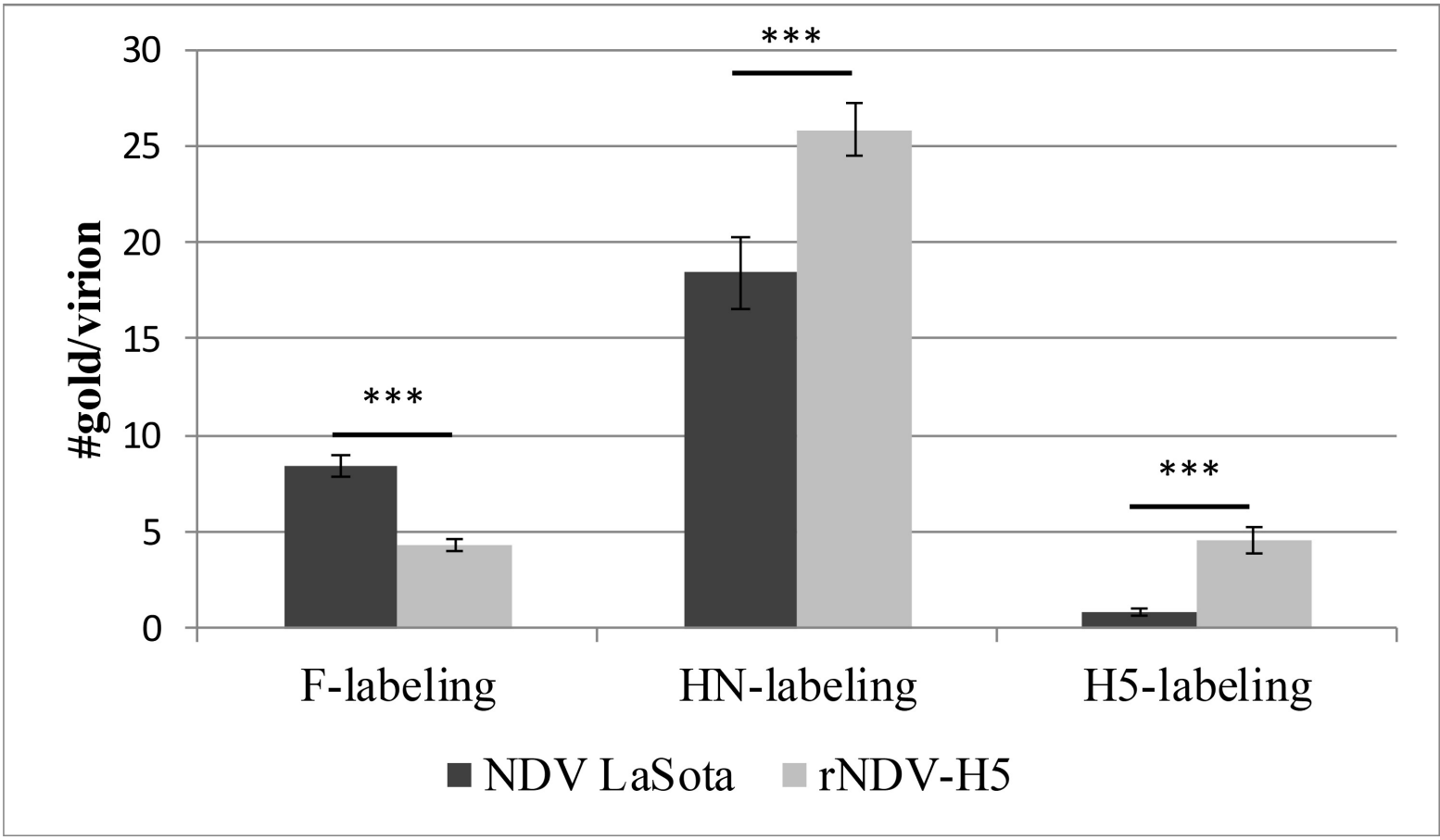
#gold/virion
30
25
20
15
10
5
0
***
***
***
F-labeling
HN-labeling
H5-labeling
NDV LaSota
rNDV-H5

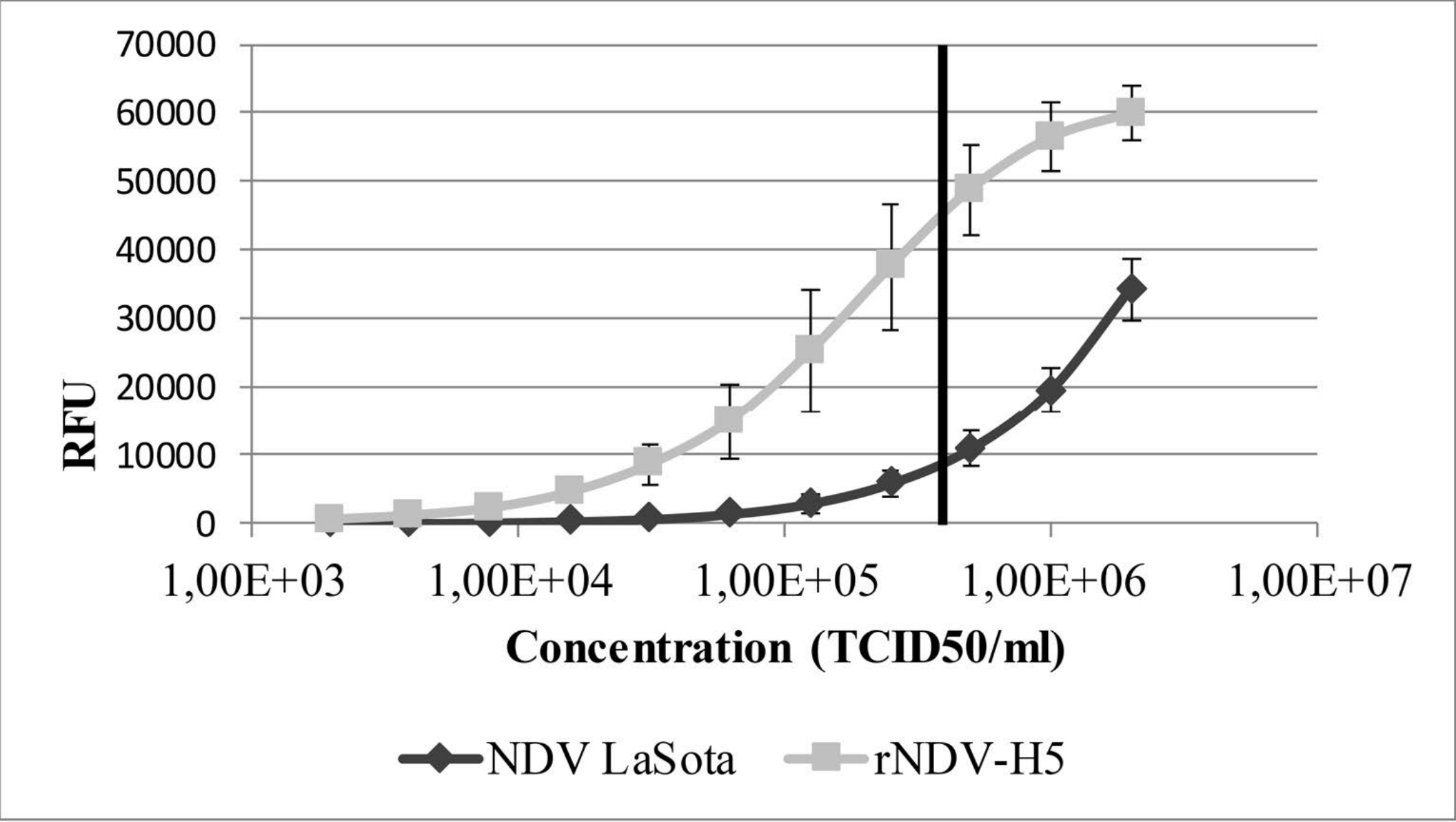
70000
60000
50000
40000
30000
20000
10000
0
RFU
1,00E+03
1,00E+04
1,00E+05
1,00E+06
1,00E+07
Concentration (TCID50/ml)
NDV LaSota
rNDV-H5

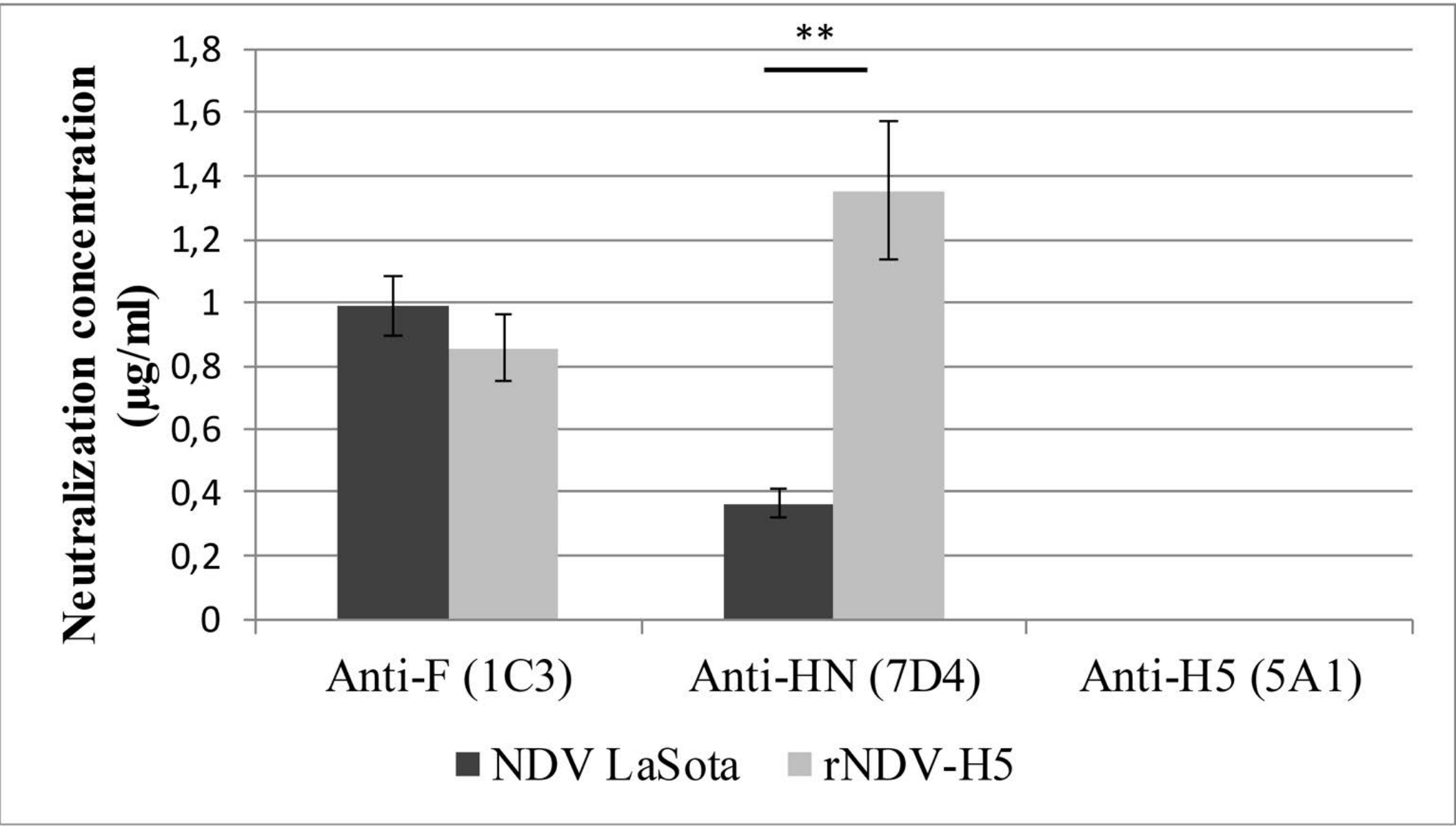
**
Neutralization concentration (µg/ml)
1,8
1,6
1,4
1,2
1
0,8
0,6
0,4
0,2
0
Anti-F (1C3)
Anti-HN (7D4)
Anti-H5 (5A1)
NDV LaSota
rNDV-H5

a)

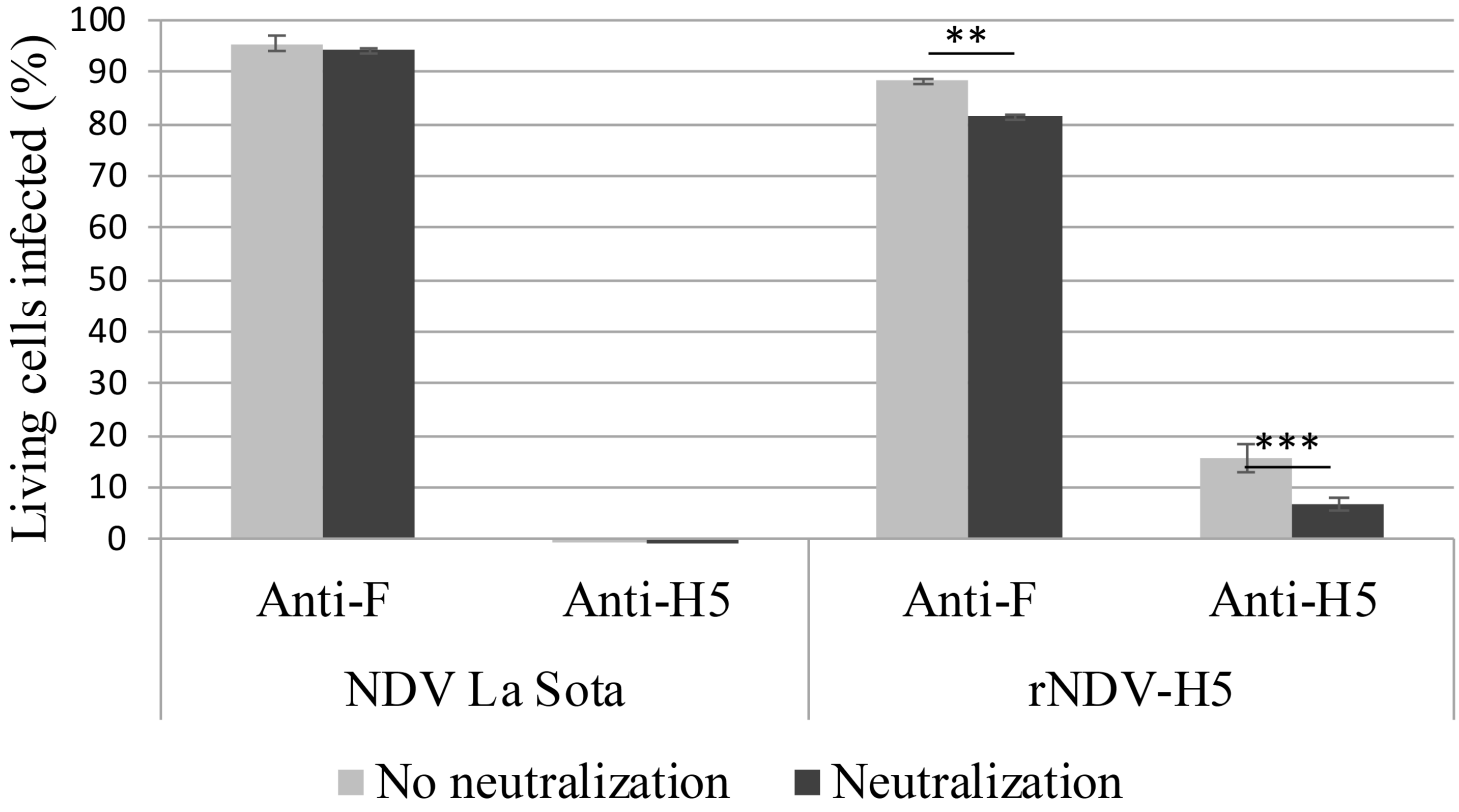
Living cells infected (%)
100
90
80
70
60
50
40
30
20
10
0
**
***
Anti-F
Anti-H5
Anti-F
Anti-H5
NDV La Sota
rNDV-H5
No neutralization
Neutralization

b)

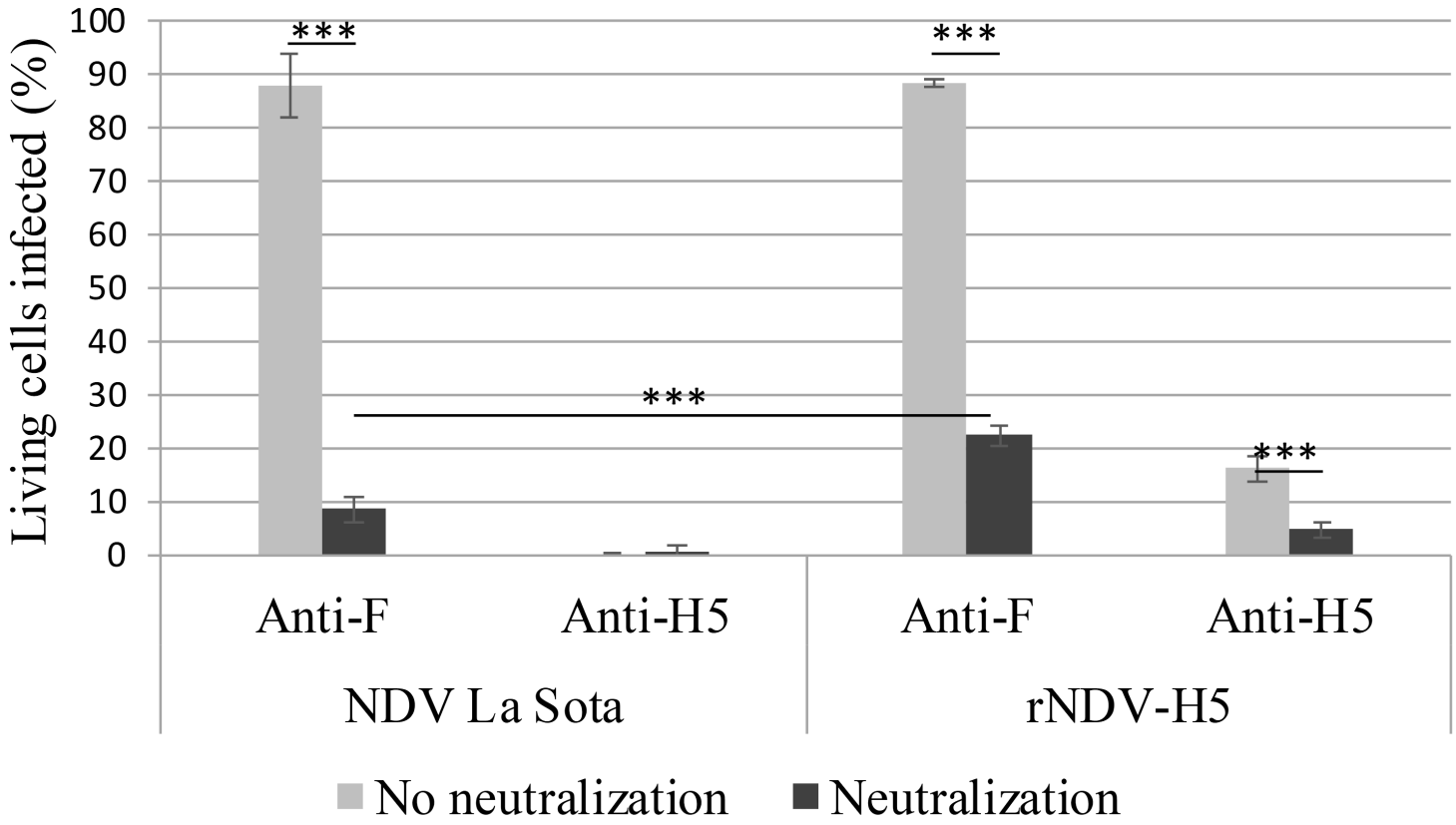
Living cells infected (%)
100
90
80
70
60
50
40
30
20
10
0
***
***
***
***
Anti-F
Anti-H5
Anti-F
Anti-H5
NDV La Sota
rNDV-H5
No neutralization
Neutralization

a)

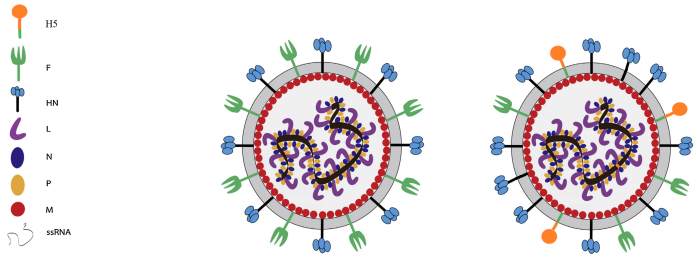
H5
F
HN
L
N
P
M
ssRNA

b)

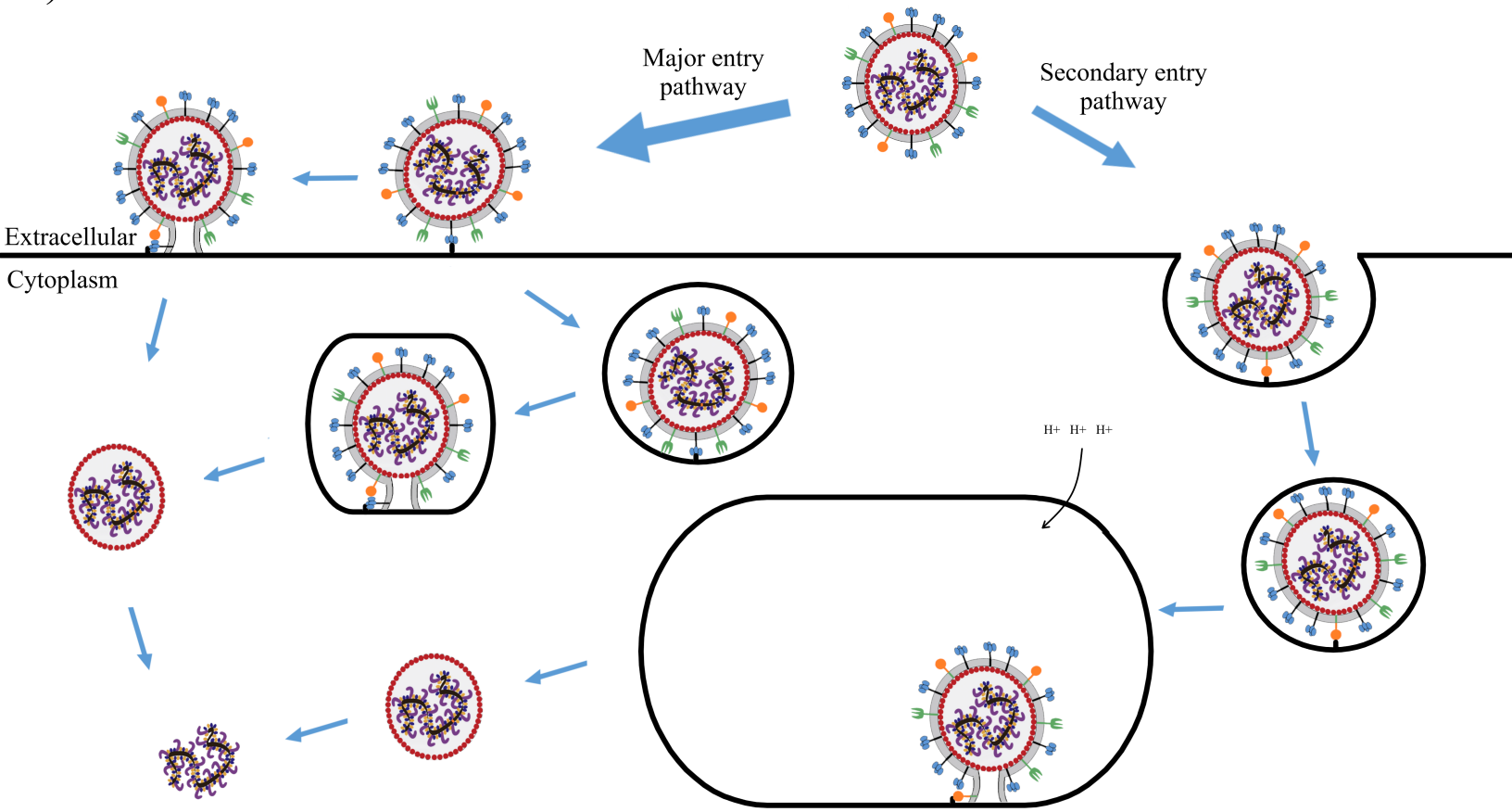
Major entry pathway
Secondary entry pathway
Extracellular
Cytoplasm
H+ H+ H+